Arabian Journal of Chemistry (2021) **14**, 103415

King Saud University

Arabian Journal of Chemistry

www.ksu.edu.sa
www.sciencedirect.com

ORIGINAL ARTICLE

Bionanocomposite of Au decorated MnO_2 via *in situ* green synthesis route and antimicrobial activity evaluation

M. Rahmat [a], H.N. Bhatti [a], A. Rehman [b], H. Chaudhry [c], M. Yameen [d,*], M. Iqbal [e,*], S.H. Al-Mijalli [f,*], N. Alwadai [g], M. Fatima [h,*], M. Abbas [i]

[a] *Department of Chemistry, University of Agriculture, Faisalabad, Pakistan*
[b] *National Institute for Biotechnology and Genetic Engineering, Faisalabad, Pakistan*
[c] *Environmental Science Department, Lahore College for Women University, Lahore, Pakistan*
[d] *Department of Biochemistry, Government College University, Faisalabad, Pakistan*
[e] *Department of Chemistry, The University of Lahore, Lahore, Pakistan*
[f] *Biology Department, College of Science, Princess Nourah bint Abdulrahman University (PNU), Riyadh, Saudi Arabia*
[g] *Department of Physics, College of Science, Princess Nourah bint Abdulrahman University (PNU), Riyadh 11671, Saudi Arabia*
[h] *Department of Physics, Deanship of Educational Services, Qassim University, Buraydah, Saudi Arabia*
[i] *Department of Biochemistry, University of Veterinary and Animal Sciences, Lahore, (Jhang Campus), Jhang 35200, Pakistan*

Received 17 May 2021; accepted 30 August 2021
Available online 06 September 2021

KEYWORDS

Bionanocomposites;
Cinnamon extract;
Manganese oxide nanofibers;
Gold nanoparticles;
Green approach;
Antimicrobial activity

Abstract Green synthesis gaining a significant importance for the preparation of nanoparticles (NPs) and NPs-based biocomposites gained much attention in biological applications. In the current study, gold (Au) nanoparticles were prepared via green approach using cinnamon extract. The Au nanocomposite (NC) was prepared with MnO_2 nanofiber mesh structure. The NC was characterized by XRD, SEM, FT-IR, EDX, UV–visible and DLS techniques. The MnO_2 nanofibers diameter was in 10–25 nm range, which was arranged in a mesh form and Au NPs was combined with nanofibers randomly. The MnO_2-Au NC antimicrobial activity was measured against *Escherichia coli*, *Pseudomonas aeruginosa* and *Staphylococcus aureus* strains. The antimicrobial activity of MnO_2-Au NC was highly promising against tested microorganisms in comparison to control (ciprofloxacin, a standard drug). The antimicrobial activity of MnO_2-Au NC was found in following order; > *S. aureus* > *E. coli* > *P. aeruginosa* with the zones inhibition of 22, 18 and 15 (mn), respectively. The MIC (minimum inhibitory concentration) values were 316, 342 and 231 (μg/mL)

* Corresponding authors.
E-mail addresses: yaminsynergic@gmail.com (M. Yameen), bosalvee@yahoo.com (M. Iqbal), shalmejale@pnu.edu.sa (S.H. Al-Mijalli), m.aziz@qu.edu.sa (M. Fatima).

Peer review under responsibility of King Saud University.

Production and hosting by Elsevier

https://doi.org/10.1016/j.arabjc.2021.103415

for *E. coli*, *P. aeruginosa* and *S. aureus,* respectively. In view of promising antimicrobial activity, the MnO_2-Au NC prepared via green approach could have potential applications in medical field and future study can be engrossed on the biocompatibility evaluation of MnO_2-Au NC using bioassays.

1. Introduction

The resistance of microbes against antibiotics is one of main factors for the inefficacy of antibiotics against infectious microorganisms, which drawn a significant consideration of researchers to develop new antimicrobial agents. In this regard, the nanotechnology meets this challenge and furnished NPs having typical properties and diverse applications in every life sphere. The noble metals-based NPs gained much attention especially for biological applications due to their ideal theragnostic aptitudes (Nazir et al., 2021; Safardoust-Hojaghan et al., 2021; Ghanbari and Salavati-Niasari, 2021) and Au NPs are ideal for biomedical applications. At current, biocomposites are gaining importance in view of their promising properties versus NPs prepared via chemical synthesis. The biocomposites have been employed successfully in the biomedical field. The Au NPs have been fabricated by employing different techniques, i.e., chemical, physical and biological routes (Karami et al., 2021; Mortazavi-Derazkola et al., 2017; Salavati-Niasari et al., 2009). Among synthesis approaches, the green route is an eco-benign and sustainable approach being used for the designing of nanomaterials since no hazardous chemical is involved during green processing versus chemically routes (Masjedi-Arani and Salavati-Niasari, 2017; Beshkar et al., 2017; Zinatloo-Ajabshir et al., 2016; Yapaoz and Attar, 2019). Different bioresources have been used to fabricate the nanomaterial, which furnished the NPs of different sizes and morphologies (Tavakoli et al., 2015; Ansari et al., 2018; Bulut Kocabas et al., 2020). Plants are the rich source of bioactive compounds like, sugars, vitamins and polyphenolics that can severe as an agent for the reduction of ions to atom and bioactive in the extract also facilitates the capping and stabilization of NPs and green route is virtuous substitute of chemical synthesis approach where templates and solvents are used (Amer and Awwad, 2021; Awwad et al., 2020; Awwad et al., 2020).

Transition metals, i.e., Ni, V, W, Mn and their oxide are widely used for synthesis of composite materials due to their physical and electrochemical properties. Among Transition metals, the MnO_2 is one of the attractive and promising material for electrochemical, magnetic and catalytic application due to its natural abundant in earth, low cost, wide potential range, nontoxic and environmentally nature. MnO_2 is also considered as promising oxidants and act as antibacterial agent, used in sensing, photocatalysis and in pharmaceuticals applications (Rahmat et al., 2019; Sanda et al., 2021; Awwad et al., 2020). The composite/doped materials facilitate the charge transmission from metals to the electronegative metal, resulting the formation of more stabilized oxidation state, which have been used for different applications, i.e., Seitz el al. (Seitz et al., 2015) prepared doped MnO_x for photocatalysis. Also, Au NPs decorated with metal showed higher catalytic activity for alcohol oxidation (Alhumaimess et al., 2014). The Au NPs deposition of metal oxide have been demonstrated to promote the oxygen evolution in a reaction . Recently, Sun et al also prepared MnO_2 composites with good catalytic activity (Sun et al., 2017) and Gorlin et al reported the deposition of Au NPs on MnOx by sputtering, which showed higher activity versus MnOx (Gorlin et al., 2014). As mention in Table 1, a lot of studies have been performed for Au NPs preparation by green for different applications. However, Cinnamon extract has not been utilized to fabricate the Au NPs. Hence, the present study was designed to prepare the Au NPs using Cinnamon extract and its composite with MnO_2 was also prepared. The as-synthesized material was studied by XRD, SEM, EDX, FTIR, UV–visible and DLS approaches. The MnO_2-Au NC antimicrobial efficacy was studied against panel of strains by disc diffusion method along with MIC.

2. Material and methods

2.1. Chemicals and reagents

2.1.1. Extract preparation

The chemical and reagents were acquired form Sigma-Aldrich. The Cinnamon extract was prepared and used for the fabrication of Au NPs. Briefly, 0.4 g of dried Cinnamon powder was dispersed in 100 mL of deionized water and heating was performed at 100 °C for 2 h. Then, the contents are filtered and resultant extract was kept at 4 °C for further use.

2.2. MnO_2-Au NC preparation

Manganese oxide nanofibrous mesh was fabricated following previously reported protocol (Tehseen et al., 2018). In a typical synthesis scheme, MnO_2 was dispersed in 100 mL deionized water and incubated at 80 °C with stirring at 600 rpm. Then during stirring, 5 mL of $HAuCl_4$ (1 M) was added and incubated for 30 min. Now, 5 mL of Cinnamon extract was supplemented and the content was incubated at 80 °C with stirring at 600 rpm. The mixture was stirred for 12000 rpm for 10 min for the separation of particle, which was washed thoroughly with deionized water several time. Finally, the sample was dried at 60 °C for 12 h and placed in a desiccator at room temperature till further analysis. The scheme for the synthesis of MnO_2-Au NC is portrayed in Fig. 1.

2.3. Characterization

The XRD spectra was recorded using X'pert Pro PAN analytical (Germany) diffractometer using CuKa radiation (λ = 1.5406A), operated at 40 kV and 30 mA in 10-80° degree range. The morphology was studied by SEM (FESEM-JSM-7500F-JEOL, Japan). Sample was prepared by dispersing powder in water (1 mg/mL) and subjected to analysis. DLS experiment was performed for determination of particle size

Table 1 Comparison of antimicrobial activity of MnO_2-Au NC with different nanomaterials and NCs.

S. No	NPs and NCs	Tested strains	ZOI (mm)	References
1	MnO_2 and Ag NPs	*E. coli, E. faecalis*	5–16	(Mahlangeni et al., 2020)
2	MnO_2 nanocolloids	*P. aeruginosa, E. coli, S. typhi*	32–35	(Rahmat et al., 2019)
3	Mn NPs	*S. aureus, E. coli*	16–24.5	(Kamran et al., 2019)
4	Zeolite\ZnO-CuO NCs	*B. subtilis*	18.9	(Alswat et al., 2017)
5	TiO_2/ZnO NCs	*S. aureus*	19.5	(Suo et al., 2019)
		E. coli	23	
6	Ag NPs	*P. aeruginosa*	10	(Ajaypraveenkumar et al., 2015)
7	MnO_2-Au NC	*E. coli*	24	Present work
		S. aureus	30	
		P. aeruginosa.	14	

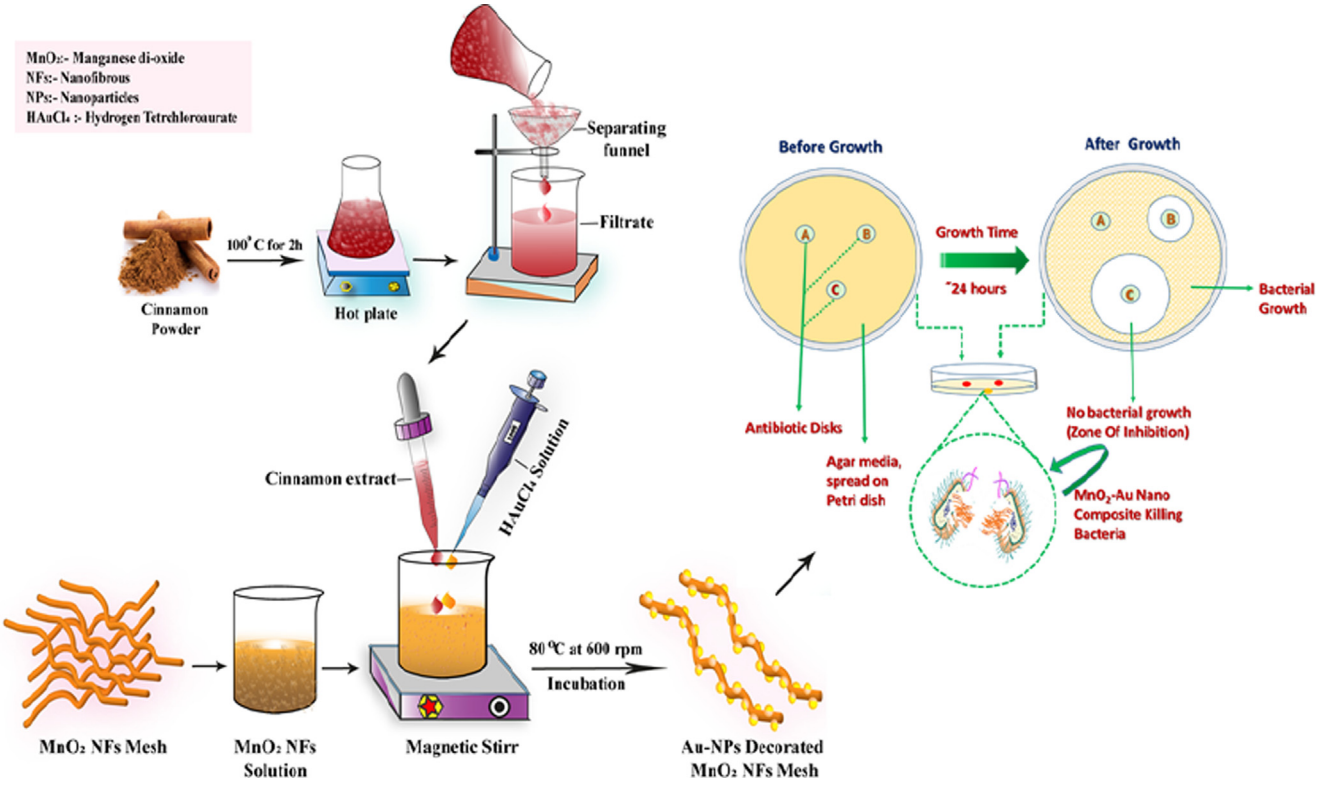

Fig. 1 Scheme adopted for the synthesis of MnO_2-Au NC.

as well as surface charge of the prepared martial (Nano-ZS; Malvern Instruments). FT-IR was used to determine the functional groups using Perkin Elmer System 2000 FT-IR spectrometer. UV–visible was performed in 200–700 nm domain (CECIL (Aquarius) 7000 series). For EDX analysis Hitachi S-4800 Japan was used.

2.4. Antimicrobial activity

The antimicrobial activity was evaluated as reported elsewhere (Rahmat et al., 2019). Antimicrobial activity was examined for *S. aureus*; *P. aeruginosa* and *E. coli* strains. The media (Nutrient agar, a growth media for bacteria) was autoclaved at 121 °C for the period of 15 min. The wicks paper discs (9 mm) were sterilized. A 20 mL media (Nutrient agar) was added in Patri plates along with 20 µL of fresh bacterial culture. The Patri plates were kept at room temperature till the media was solidified. With the help of forcep, disc containing 500 µL MnO_2-Au NC (50 mg/mL) were placed flat on the medium (growth media) and Petri plates were incubated at 37 °C for 24 h. The NC inhibited the bacterial growth, which was recorded with zone reader in mm. All the run was performed in triplicate and data obtained was averaged. For the measurement of MIC, the method reported elsewhere was followed (Sarker et al., 2007).

3. Results and discussion

3.1. XRD analysis

The structural analysis was performed by XRD study and response thus obtained is shown in Fig. 2. The peaks recorded

were of 220, 300, 211, 420, 521, 202 and 312 indices and matched precisely with JCPDS card no. 44-0141. No extra peaks were observed, which indicate the purity of prepared material. The composite showed a peak of Au in addition to the MnO_2, which is an indication of MnO_2 composite formation with Au. Also, these findings are in line with reported studies, i.e., a hydrothermal treatment was adopted for the fabrication of MnO_2 by (Hlaing and Win, 2012) and a very uniform MnO2 nanorods with diameters of 30–50 nm were obtained under control of conditions (temperature and reaction time). Also, PLAL has been used for the fabrication of MnO_2 NCs. The PLAL furnished high crystalline MnO2 NCs with crystallite size of 52 nm (Rahmat et al., 2019).

3.2. UV–Vis analysis

The MnO_2-Au NC UV–Vis was performed in 200 to 800 nm range and response this observed is presented in Fig. 3. In UV–Vis absorption spectrum, two characteristic peaks were observed at 245 nm and 490 nm, which are corelated with MnO_2 and Au, respectively. The visual appearance of ruby red color also reveals the formation of Au nanoparticles. The absorption bands in 197–270 nm and 450–785 nm range were recorded in case of MnO_2, while in case of MnO_2-Au NC, the intensity of the absorption peak in 450–785 nm range reduced significantly, which is indication of interaction Au with MnO_2 in NC formation.

3.3. DLS analysis

The dynamic light scattering (DLS) is an analytical tool used to measure the hydrodynamic diameter of NPs in liquid medium. It also provides information about the surface charge of the fabricated materials. The zeta potential of the MnO_2 nanofibers mesh was −26.3 mV (Fig. 4a). The negative values revealed the higher stability of the NC (Liu et al., 2014). Moreover, a reduction in value of zeta potential was observed in MnO_2-Au, i.e., −12.2 mV (Fig. 4b), which is also an indication of NC formation of MnO_2 and Au NPs.

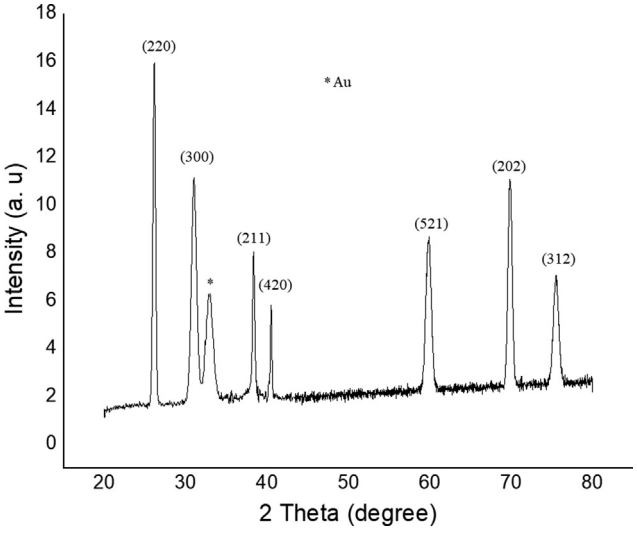

Fig. 2 XRD pattern of MnO_2-Au NC.

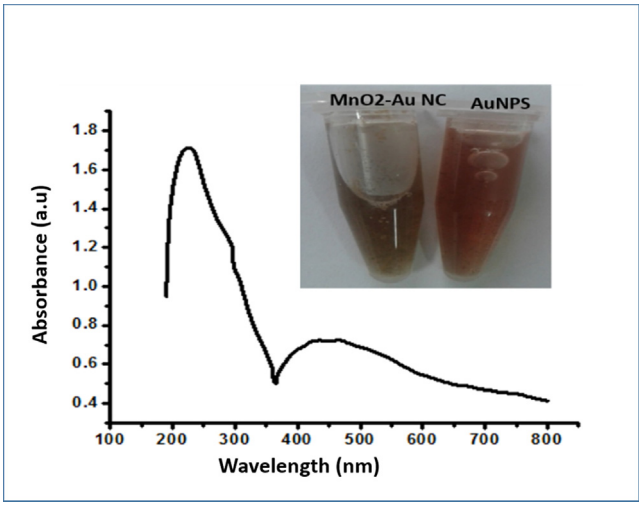

Fig. 3 UV–VIS spectrum of MnO_2-Au NC.

3.4. FT-IR analysis

FT-IR spectra of MnO_2 nanofiber mesh and MnO_2-Au NPs NC are shown in Fig. 5. In the spectra, a characteristic peak of MnO is observe at 570 and 690 (cm^{-1}). In case of MnO_2-Au NPs NC, a band at 3321 cm^{-1} was observed due to OH stretching vibration. The band observed at 1053 cm^{-1} was assigned to the —CO— stretching. A band at 1634 cm^{-1} is due to —C═C— stretching and bending at 2127 cm^{-1} is due to C—H functional group. The analysis revealed that Cinnamon extract comprises a variety of phytochemicals, which are responsible for the reduction, stabilizing of Au atom (Fig. 6). Moreover, in comparison to the MnO_2 nanofiber, a band at 570 and 690 (cm^{-1}) are due to Mn-O bending vibration. While for MnO_2-Au NPs NC, the absorption bands are shifted slightly (blue shift) to 668 and 707 (cm^{-1}), respectively, which is due to interaction between Au NPs and MnO_2 nanofibers. These results are also in line with reported studies, where the interaction of the hydroxyl group (O—H) with Mn atoms is documented. The peaks appeared at 665, 641, and 611 (cm^{-1}) were corelated with Mn—O bonding. With the growth of Au NPs on the surface of Mn—O, the absorption bands shifted to 1682, 670, 645 (cm^{-1}) revealed the successfully incorporation of Au atoms on the surface of MnO_2 nanofibers.

3.5. Surface morphology

The properties of the NPs depend on the morphology and size of the particles. Hence, the morphology was studied by FE-SEM and outcome is portrayed in Fig. 7a. The MnO_2 formed a nanofiber structure and the fibers diameter was in 10–25 nm range and length was several microns. The length to diameter ratio was found to be enough high, which reveals the fibrous morphology. Moreover, the MnO_2 forms a mesh like structure and the pores of the meshes were in 10–500 nm range. The fibers are highly flexible due to their extra-long length, which makes the loops and curves in the fibers. The mesh structure has various advantages like it has high surface area, mesh precludes the fibers from aggregation, which resultantly may offer high activity during catalytic and photocatalytic activity. The

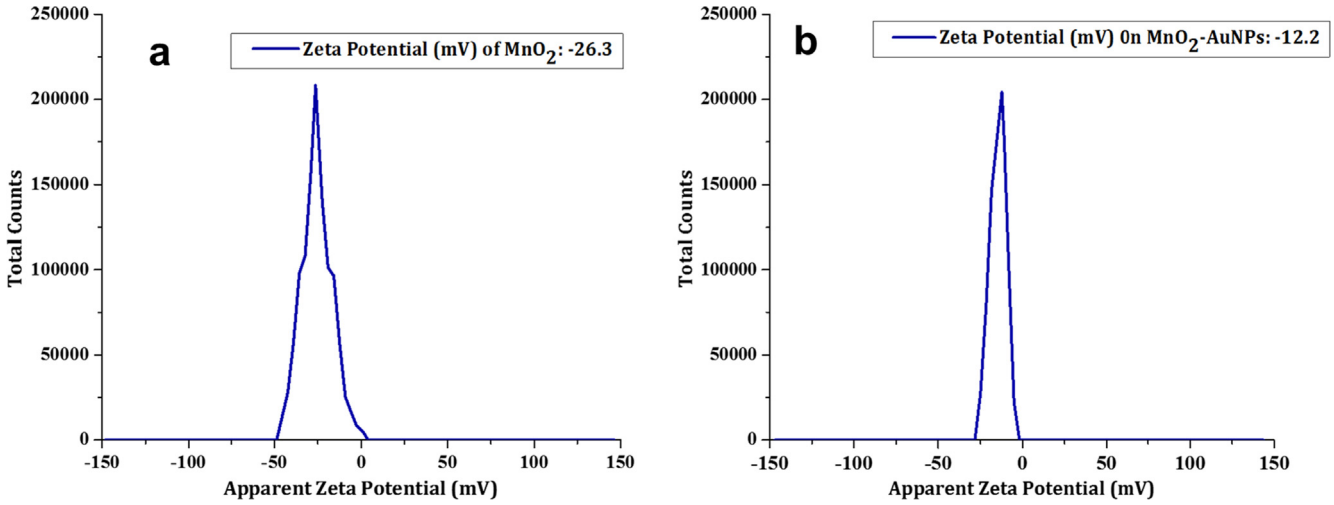

Fig. 4 (a) Zeta potential of MnO_2 and (b) MnO_2-Au NC.

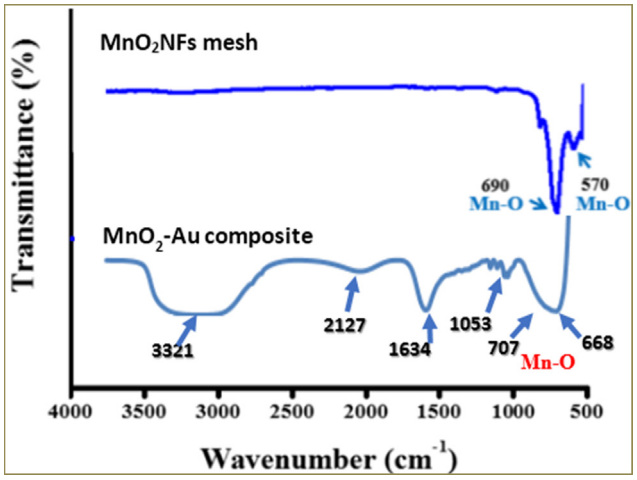

Fig. 5 FT-IR spectra of MnO_2 NFs mesh and MnO_2-Au NC.

average diameter of Au NPs was estimated to be 14 nm (Fig. 7-a-d), which are randomly distributed over the surface of the MnO_2 nanofibers. Au NPs with high electronegativity can affect the physicochemical attributes of MnO_2 nanofibers due to ideal surface-to-volume ratio (Liu et al., 2014).

3.6. Elemental analysis

The elemental composition of the MnO_2-Au NC was studied by EDX analysis and response this obtained is depicted in Fig. 8. The EDX analysis furnished data, which contains peaks corresponding to the elemental composition of the sample being analyzed. EDX spectrum of MnO_2-Au NC depicts the presence of C, O, Mn and Au elements. No peak for impurity was observed ensuring purity of the prepared composite material. It can be concluded that a successful decoration of Au NPs was achieved on MnO_2 nanofiber mesh structure. The Mn and Au proportion in the NC was 10.14 and 1.94 (%), respectively. The findings revealed that the MnO_2-Au NC fabricated are in highly pure form since no additional peaks are detected in the EDX spectrum.

3.7. Antimicrobial activity

The MnO_2-Au NC antimicrobial activity was assessed against three microbial strains, which was compared with standard antibiotic ciprofloxacin. The antimicrobial activity of MnO_2-Au NPs NC was perfumed versus *S. aureus*, *P. aeruginosa* and *E. coli* strains and responses are presented Fig. 9. The ciprofloxacin was used as a standard to compare the antimicrobial activity of MnO_2-Au NPs. The MnO_2-Au NPs showed excellent antimicrobial activity against selected microbes and the zones of inhibition were in following order; *S. aureus* > *E. coli* > *P. aeruginosa*. The zones of inhibition in case of *S. aureus, E. coli* and *P. aeruginosa* were recorded to be 22, 18 and 15 (mm), respectively, whereas this value was 32–36 mm in case of ciprofloxacin in case of *S. aureus, E. coli* and *P. aeruginosa*. Previous studies also supports the findings of present investigation that composite based are good antimicrobial agents, i.e., *E. coli* growth was significantly inhibited by the Ag/MnO_2 NCs (Rahmat et al., 2019). Also, Ag doped MnO_2 showed promising activity against *S.* aureus, *S.* epidermis, *B.* subtilis, *E. coli*, *S. abony* and *K. pneumonia* strains (Kunkalekar et al., 2014). Similarly, CS-MnO_2 also furnished auspicious antimicrobial activity against panel of microbial strain (Anwar, 2018) and ternary nanocomposite of MnO_2 also showed auspicious activity against *E. coli* and *S. aureus* strains (Venkatesh et al., 2017). Also, present investigation revealed that the MnO_2-Au NC is highly active antimicrobial agent, which could have potential biological application as an antimicrobial agent (Table 1). Previous studies showed that TiO_2/ZnO NCs and ZnO NPs, the MnO_2-Au NC showed higher antimicrobial activity. In comparison to Ag NPs along, the MnO_2-Au NC also showed higher efficiency.

The MIC was also studied of MnO_2-Au NC against *S. aureus, P. aeruginosa* and *E. coli* and results are portrayed in Fig. 10. The MIC value is the considered the lowest concentration of the tested compound, which inhibited the microbial growth (no growth observed at MIC value). The MIC values were found to be in line with the antibacterial activity. The MIC value was 231 μg/mL (lowest) in case of *S. aureus*, whereas this value was 316 μg/mL for *E. coli* and 342 μg/mL in case of *P. aeruginosa*. The standard antibiotic (ciprofloxa-

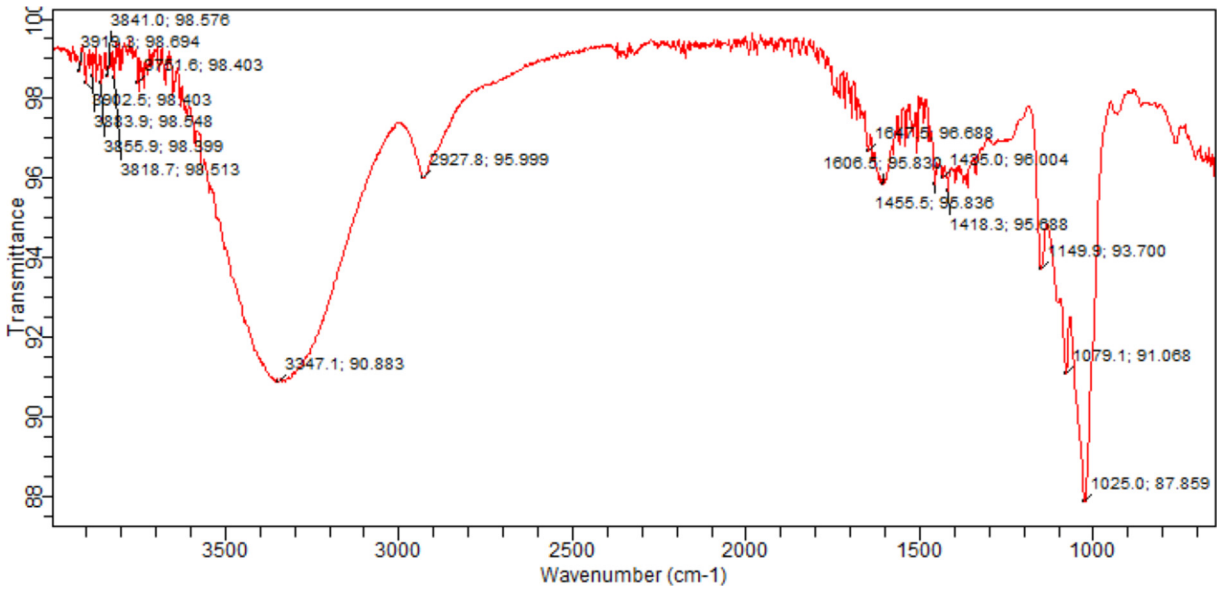

Fig. 6 FT-IR spectra of extract used for the preparation of Au NPs.

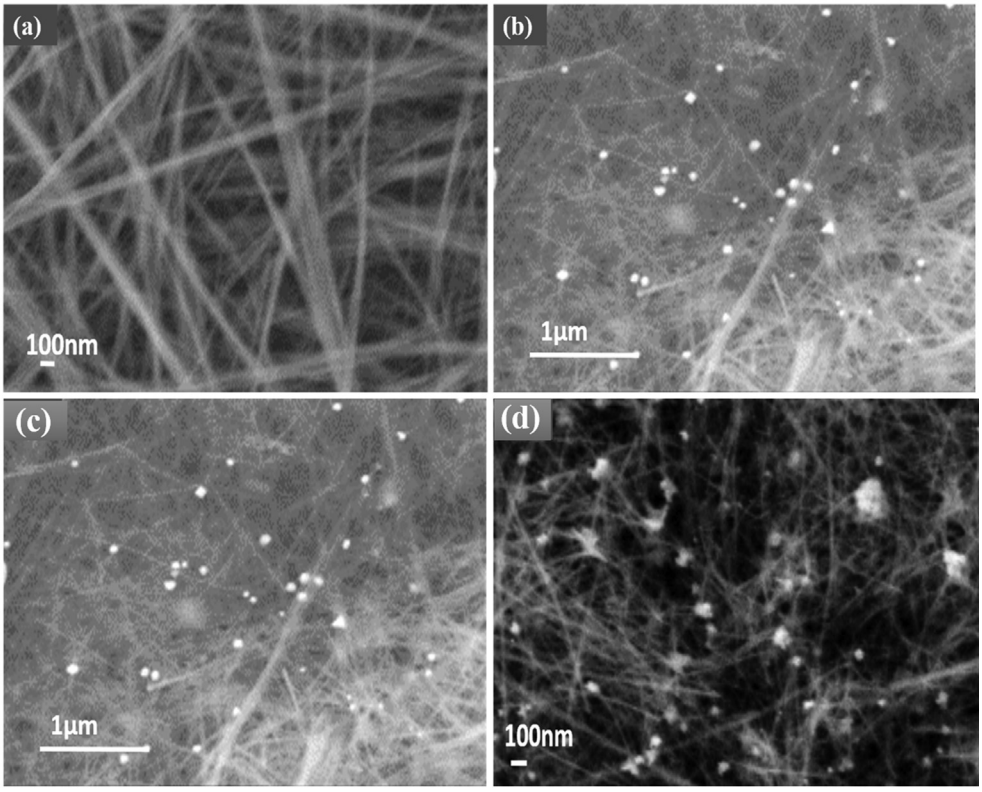

Fig. 7 FE-SEM analysis, (a) MnO_2 nanofibers and (b-d) MnO_2-Au NC.

cin) showed the MIC values 105, 126 and 61 (µg/mL) against *E. coli, P. aeruginosa* and *S. aureus,* respectively. The higher antibacterial activity is due to the different interactive effect of MnO_2-Au NC with microbial cell due to ions formation and reactive oxygen species (ROS) generation, which collectively leads to cell to death (Fig. 11). The antibacterial activity of the NPs depends upon various factors, i.e., absorption rate, release of metabolites, metabolic functions and distribution in the cell. The NPs binds with the cell of microorganism, attached with the surface through active moieties and then, diffused inside the cell and interactive with the cell different components. For example, if the NPs binds/interact with proteins, which is an important biomolecule in cell to perform different functions, i.e., it takes part in the formation of cell wall, ribo-

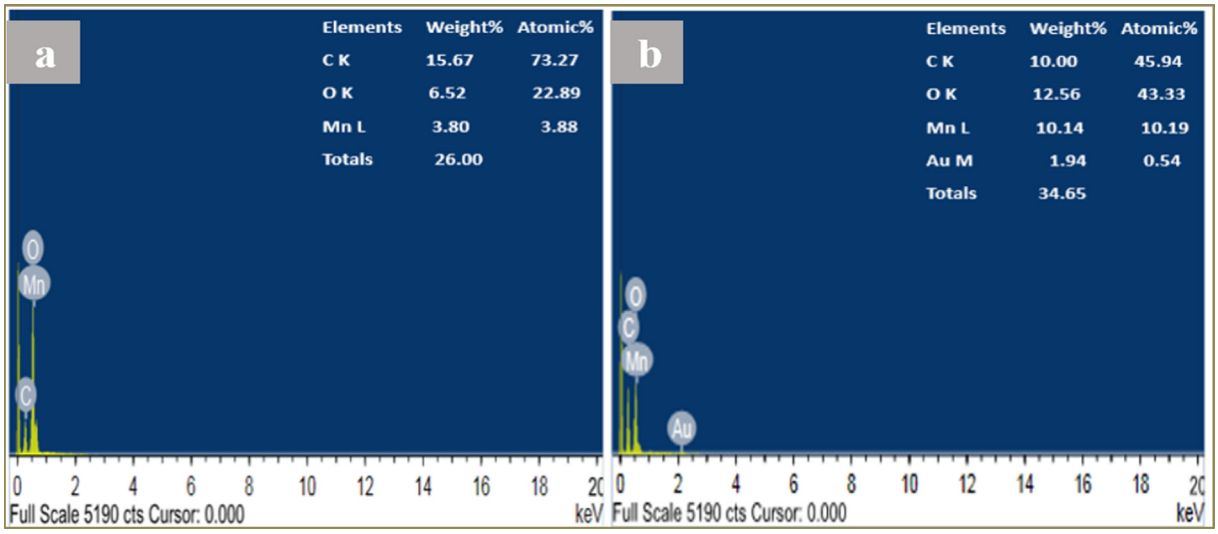

Fig. 8 (a) EDX analysis of MnO_2 nanofibers and (b) MnO_2-Au NC.

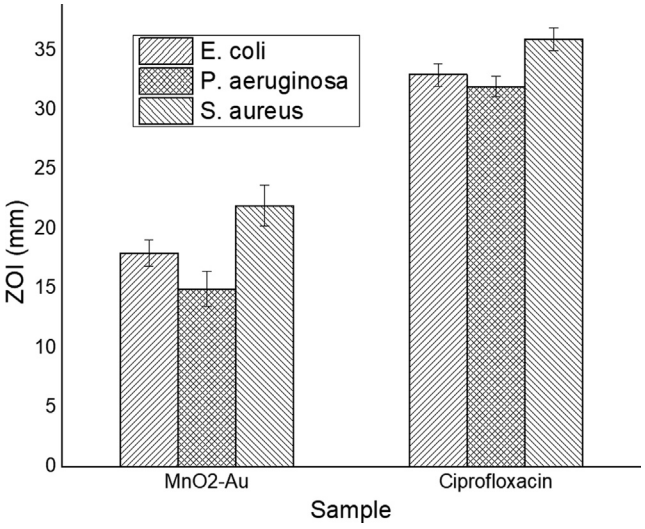

Fig. 9 Antimicrobial activity (zone of inhibition) of MnO_2-Au NC.

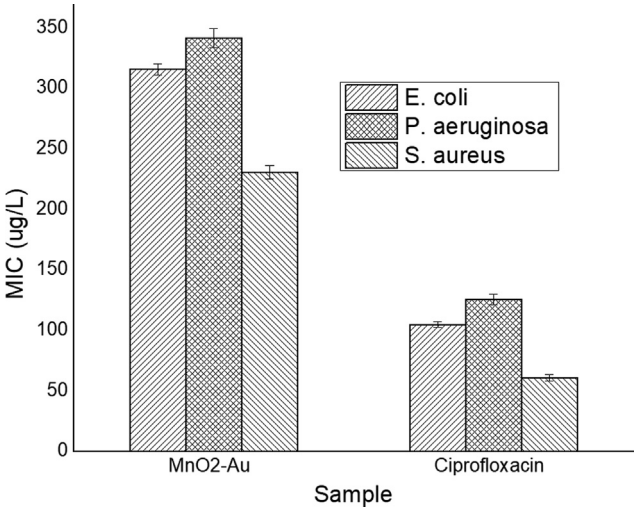

Fig. 10 Minimum inhibitory concentration (MIC, μg/mL) MnO_2-Au NC.

somes, cell membrane and nucleic acids and if protein synthesis is inhibited inside the cell and them, all activities related to protein are stopped and resultantly, cell death occur. The overall proposed antimicrobial mechanism is explained in Fig. 10. The binds with cell wall of microbe, penetrates into cell membrane and cause membrane destruction and disrupt (proteins, enzymes, and DNA). The NPs produce ROS inside the cell and these ROS induce oxidative stress and resultantly, metabolic pathways are disturbed and cell occurred.

The antibacterial activity of the NPs depends upon various factors, i.e., absorption rate, release of metabolites, metabolic functions and distribution in the cell. The NPs binds with the cell of microorganism, attached with the surface through active moieties and then, diffused inside the cell and interactive with the cell different components. For example, if the NPs binds/interact with proteins, which is an important biomolecule in cell to perform different functions, i.e., it takes part in the formation of cell components (wall, membrane, ribosome and nucleic acids) and if protein synthesis is inhibited inside the cell and them, all activities related to protein are stopped and resultantly, cell death occur. The overall proposed antimicrobial mechanism is explained in Fig. 10. The binds with cell wall of microbe, penetrates into cell membrane and cause membrane destruction and disrupt (proteins, enzymes, and DNA). The NPs produce ROS inside the cell and these ROS induce oxidative stress and resultantly, metabolic pathways are disturbed and cell occurred. These ROS include hydroxyl radicals ($OH^{\cdot}$), and superoxide ions $O_2^{-\cdot}$ These free radicals interact with biomolecules, which disintegrate the plasma membrane and cause lipid oxidation. The hydrogen peroxide produced cause toxicity to the cell and ultimately, leads to the cell death (Sharma et al., 2021). The NPs and NC prepared promising antibacterial activity versus related nanomaterials prepared chemical methods. Hence, the adoption of green route is more feasible to prepare the NPs (Awwad et al.,

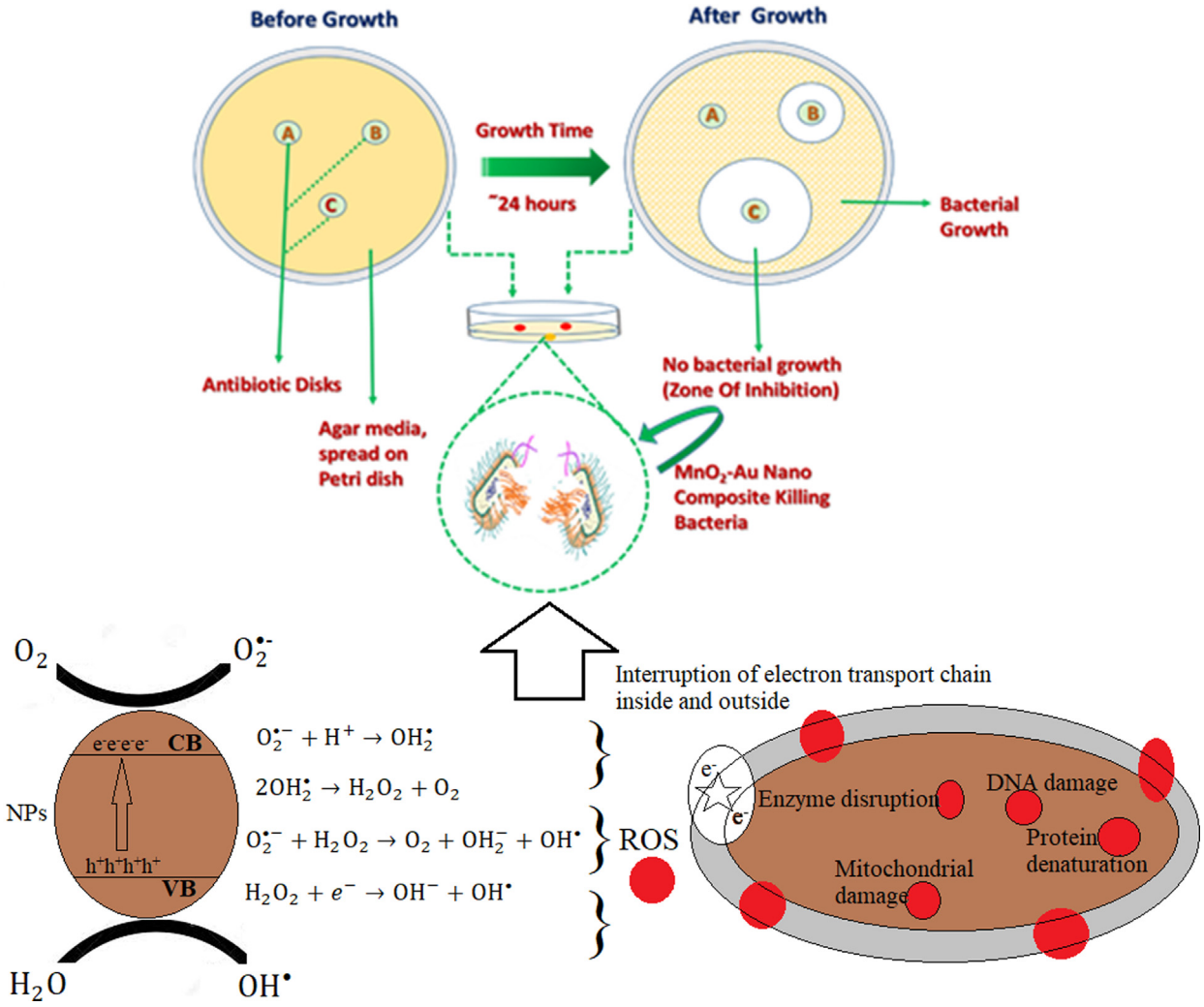

Fig. 11 Antimicrobial activity mechanism of MnO_2-Au NC.

2020; Awwad et al., 2020; Awwad and Amer, 2020; Al Banna et al., 2020; Igwe and Nwamezie, 2018; Remya et al., 2017) and their composites for biomedical applications.

4. Conclusions

The Au NPs was prepared by green route using cinnamon extract and nanocomposite of Au was prepared with MnO_2 nanofibrous mesh. The characteristics of MnO_2-Au NC was studied by SEM, XRD, FT-IR, EDX, UV–visible and DLS techniques. The MnO_2 nanofibers diameter was in 10–25 mm range. The length to diameter ratio was found to be enough high, which reveals the fibrous morphology. The MnO_2 forms a mesh like structure and the pores of the meshes were in 10–500 nm range and Au atom was distributed randomly on the surface of nanofibers. The MnO_2-Au NC showed promising antimicrobial activity against *S. aureus, E. coli* and *P. aeruginosa*. The MIC values were 231–342 μg/mL range for *E. coli*, *P. aeruginosa* and *S. aureus,* respectively. The MnO_2-Au NC furnished auspicious. In view of promising antimicrobial activity and could have potential applications in medical field, which need further studied for the evaluation of biocompatibility of MnO_2-Au NC.

Declaration of Competing Interest

The authors declare that they have no known competing financial interests or personal relationships that could have appeared to influence the work reported in this paper.

Acknowledgement

This research was funded by the Deanship of Scientific Research at Princess Nourah bint Abdulrahman University through the Fast-track Research Funding Program.

Reference

Ajaypraveenkumar, Arockiasamy, Henry, Johnson, Mohanraj, Kannusamy, Sivakumar, Ganesan, Umamaheswari, Sankaran, 2015. Characterisation, luminescence and antibacterial properties of stable agnps synthesised from AgCl by precipitation method. J. Mater. Sci. Technol. 31 (11), 1125–1132.

Al Banna, L.S., Salem, N.M., Jaleel, G.A., Awwad, A.M., 2020. Green synthesis of sulfur nanoparticles using Rosmarinus officinalis leaves extract and nematicidal activity against *Meloidogyne javanica*. Chem. Int. 6 (3), 137–143.

Alhumaimess, Mosaed, Lin, Zhongjie, He, Qian, Lu, Li, Dimitratos, Nickolaos, Dummer, Nicholas F., Conte, Marco, Taylor, Stuart H., Bartley, Jonathan K., Kiely, Christopher J., Hutchings, Graham J., 2014. Oxidation of benzyl alcohol and carbon monoxide using gold nanoparticles supported on MnO2 nanowire microspheres. Chem. Eur. J. 20 (6), 1701–1710.

Alswat, Abdullah A, Ahmad, Mansor Bin, Saleh, Tawfik A., 2017. Preparation and characterization of zeolite\zinc oxide-copper oxide nanocomposite: Antibacterial activities. Colloid Interf. Sci. Commun. 16, 19–24.

Amer, M.W., Awwad, A.M., 2021. Green synthesis of copper nanoparticles by *Citrus limon* fruits extract, characterization and antibacterial activity. Chem. Int. 7 (1), 1–8.

Ansari, Fatemeh, Sobhani, Azam, Salavati-Niasari, Masoud, 2018. Simple sol-gel synthesis and characterization of new $CoTiO_3$/$CoFe_2O_4$ nanocomposite by using liquid glucose, maltose and starch as fuel, capping and reducing agents. J. Colloid Interf. Sci. 514, 723–732.

Anwar, Yasir, 2018. Antibacterial and lead ions adsorption characteristics of chitosan-manganese dioxide bionanocomposite. Int. J. Biol. Macromol. 111, 1140–1145.

Awwad, A.M., Amer, M.W., Al-Aqarbeh, M.M., 2020. TiO_2-kaolinite nanocomposite prepared from the Jordanian Kaolin clay: Adsorption and thermodynamic of Pb(II) and Cd(II) ions in aqueous solution. Chem. Int. 6 (4), 168–178.

Awwad, A.M., Amer, M.W., Salem, N.M., Abdeen, A.O., 2020. Green synthesis of zinc oxide nanoparticles (ZnO-NPs) using Ailanthus altissima fruit extracts and antibacterial activity. Chem. Int. 6 (3), 151–159.

Awwad, A.M., Amer, M.W., 2020. Biosynthesis of copper oxide nanoparticles using *Ailanthus altissima* leaf extract and antibacterial activity. Chem. Int. 6 (4), 210–217.

Awwad, A.M., Salem, N.M., Aqarbeh, M.M., Abdulaziz, F.M., 2020. Green synthesis, characterization of silver sulfide nanoparticles and antibacterial activity evaluation. Chem. Int. 6 (1), 42–48.

Beshkar, Farshad, Khojasteh, Hossein, Salavati-Niasari, Masoud, 2017. Recyclable magnetic superhydrophobic straw soot sponge for highly efficient oil/water separation. J. colloid Interf. Sci. 497, 57–65.

B. Bulut Kocabas, A. Attar, A. Peksel, M.J.B. Altikatoglu Yapaoz, A. Biochemistry, phytosynthesis of CuONPs via Laurus nobilis: Determination of antioxidant content, antibacterial activity, and dye decolorization potential, Biotechnol. Appl. Biochem. 69 (2020) 1–10.

Ghanbari, M., Salavati-Niasari, M., 2021. Copper iodide decorated graphitic carbon nitride sheets with enhanced visible-light response for photocatalytic organic pollutant removal and antibacterial activities. Ecotoxicol. Environ. Saf. 208, 111712.

Gorlin, Yelena, Chung, Chia-Jung, Benck, Jesse D., Nordlund, Dennis, Seitz, Linsey, Weng, Tsu-Chien, Sokaras, Dimosthenis, Clemens, Bruce M., Jaramillo, Thomas F., 2014. Understanding interactions between manganese oxide and gold that lead to enhanced activity for electrocatalytic water oxidation. J. Am. Chem. Soc. 136 (13), 4920–4926.

Hlaing, A.A., Win, P.P., 2012. The synthesis of α-MnO_2 nanorods using hydrothermal homogeneous precipitation, dvances in Natural Sciences: Nanosci. Nanotechnol. 3, (2) 025001.

Igwe, O.U., Nwamezie, F., 2018. Green synthesis of iron nanoparticles using flower extract of *Piliostigma thonningii* and antibacterial activity evaluation. Chem. Int. 4, 60–66.

Kamran, Urooj, Bhatti, Haq Nawaz, Iqbal, Munawar, Jamil, Saba, Zahid, Muhammad, 2019. Biogenic synthesis, characterization and investigation of photocatalytic and antimicrobial activity of manganese nanoparticles synthesized from Cinnamomum verum bark extract. J. Mol. Struct. 1179, 532–539.

Karami, Maryam, Ghanbari, Mojgan, Alshamsi, Hassan Abbas, Rashki, Somaye, Salavati-Niasari, Masoud, 2021. Facile fabrication of Tl 4 HgI 6 nanostructures as novel antibacterial and antibiofilm agents and photocatalysts in the degradation of organic pollutants. Inorgan. Chem. Front. 8 (10), 2442–2460.

Kunkalekar, R.K., Prabhu, M.S., Naik, M.M., Salker, A.V., 2014. Silver-doped manganese dioxide and trioxide nanoparticles inhibit both gram positive and gram negative pathogenic bacteria. Colloid. Surf. B 113, 429–434.

Liu, Xijun, Liu, Junfeng, Li, Yaping, Li, Yingjie, Sun, Xiaoming, 2014. Au/$NiCo_2O_4$ arrays with high activity for water oxidation. Chem. Cat. Chem. 6 (9), 2501–2506.

Mahlangeni, Nomfundo T., Magura, Judie, Moodley, Roshila, Baijnath, Himansu, Chenia, Hafizah, 2020. Biogenic synthesis, antioxidant and antimicrobial activity of silver and manganese dioxide nanoparticles using *Cussonia zuluensis* Strey. Chem, Paper. 74 (12), 4253–4265.

Masjedi-Arani, Maryam, Salavati-Niasari, Masoud, 2017. Novel synthesis of Zn_2GeO_4/graphene nanocomposite for enhanced electrochemical hydrogen storage performance. Int. J. Hydrog. Energy 42 (27), 17184–17191.

Mortazavi-Derazkola, Sobhan, Salavati-Niasari, Masoud, Amiri, Omid, Abbasi, Ali, 2017. Fabrication and characterization of Fe_3O_4@SiO_2@ TiO_2@Ho nanostructures as a novel and highly efficient photocatalyst for degradation of organic pollution. J. Energy Chem. 26 (1), 17–23.

Nazir, A., Akbar, A., Baghdadi, H.B., ur Rehman, S., Al-Abbad, E., Fatima, M., Iqbal, M., Tamam, N., Alwadai, N., Abbas, M., 2021. Zinc oxide nanoparticles fabrication using Eriobotrya japonica leaves extract: Photocatalytic performance and antibacterial activity evaluation. Arab. J. Chem. 14 (8). 103251.

Rahmat, M., Rehman, A., Rahmat, S., Bhatti, H.N., Iqbal, M., Khan, W.S., Jamil, Y., Bajwa, S.Z., Sarwar, Y., Rasul, S., 2019. Laser ablation assisted preparation of MnO_2 nanocolloids from waste battery cell powder: Evaluation of physico-chemical, electrical and biological properties. J. Mol. Struct. 1191, 284–290.

Remya, V., Abitha, V., Rajput, P., Rane, A., Dutta, A., 2017. Silver nanoparticles green synthesis: a mini review. Chem. Int. 3 (2), 165–171.

Safardoust-Hojaghan, Hossein, Salavati-Niasari, Masoud, Amiri, Omid, Rashki, Somaye, Ashrafi, Mahdi, 2021. Green synthesis, characterization and antimicrobial activity of carbon quantum dots-decorated ZnO nanoparticles. Ceram. Int. 47 (4), 5187–5197.

Salavati-Niasari, Masoud, Fereshteh, Zeinab, Davar, Fatemeh, 2009. Synthesis of oleylamine capped copper nanocrystals via thermal reduction of a new precursor. Polyhedron 28 (1), 126–130.

Sanda, M.D.A., Badu, M., Awudza, J.A., Boadi, N.O., 2021. Development of TiO_2-based dye-sensitized solar cells using natural dyes extracted from some plant-based materials. Chem. Int. 7 (1), 9–20.

Sarker, Satyajit D., Nahar, Lutfun, Kumarasamy, Yashodharan, 2007. Microtitre plate-based antibacterial assay incorporating resazurin as an indicator of cell growth, and its application in the in vitro antibacterial screening of phytochemicals. Methods 42 (4), 321–324.

Seitz, L.C., Hersbach, T.J., Nordlund, D., Jaramillo, T.F., 2015. Enhancement effect of noble metals on manganese oxide for the oxygen evolution reaction. J. Phys. Chem. Lett. 6 (20), 4178–4183.

Sharma, D., Shandilya, P., Saini, N.K., Singh, P., Thakur, V.K., Saini, R.V., Mittal, D., Chandan, G., Saini, V., Saini, A.K., 2021. Insights into the synthesis and mechanism of green synthesized antimicrobial nanoparticles, answer to the multidrug resistance. Mater. Today Chem. 19, 100391.

Sun, Lijun, Li, Jin, Cai, Jun, Zhong, Lian, Ren, Guohui, Ma, Qimin, 2017. One pot synthesis of gold nanoparticles using chitosan with

varying degree of deacetylation and molecular weight. Carbohyd. Polym. 178, 105–114.

Suo, Hao, Peng, Changxin, Jing, Feng, Yu, Shuwen, Cui, Sheng, Shen, Xiaodong, 2019. Facile preparation of TiO_2/ZnO composite aerogel with excellent antibacterial activities. Mater. Lett. 234, 253–256.

Tavakoli, Farnosh, Salavati-Niasari, Masoud, badiei, Alireza, Mohandes, Fatemeh, 2015. Green synthesis and characterization of graphene nanosheets. Mater. Res. Bull. 63, 51–57.

Tehseen, Bushra, Rehman, Asma, Rahmat, Muniba, Bhatti, Haq Nawaz, Wu, Aiguo, Butt, Faheem K., Naz, Gul, Khan, Waheed S., Bajwa, Sadia Z., 2018. Solution growth of 3D MnO_2 mesh comprising 1D nanofibres as a novel sensor for selective and sensitive detection of biomolecules. Biosens. Bioelectron. 117, 852–859.

Venkatesh, T., Mahesh, K.V., Mylarappa, M., Siddeswara, D., Raghavendra, N., Kumar, M.S., Rangappa, D., Prasanna, D., 2017. Facile synthesis and characterization of MnO_2/-graphene/multi walled carbon nanotube nanostructured ternary composite: an advance material for environmental and biological applications. Mater. Today: Proc. 4 (11), 11915–11922.

Yapaoz, M.A., Attar, A., 2019. Salvia officinalis-derived rutile TiO_2-NPs: production, characterization, antibacterial evaluation and its effect on decolorization. Mater. Res. Exp. 6, (5) 055039.

Zinatloo-Ajabshir, S., Salavati-Niasari, M., Zinatloo-Ajabshir, Z., 2016. $Nd_2Zr_2O_7$-Nd_2O_3 nanocomposites: new facile synthesis, characterization and investigation of photocatalytic behaviour. Mater. Lett. 180, 27–30.